

## AN INVESTIGATION OF METAL TRANSFER PROCESS IN GMAW

M. S. Węglowski<sup>1)</sup>, Y. Huang<sup>2)</sup>, Y. M. Zhang<sup>2)</sup>

<sup>1)</sup> **Institute of Welding**

**Testing of Materials Weldability and Welded Constructions Department**

Bl. Czesława 16/18, 44-100 Gliwice, Poland

<sup>2)</sup> **University of Kentucky**

**Center for Manufacturing**

Lexington, KY 40506, USA

This paper presents the studies of the metal transfer process in gas metal arc welding with mild steel electrode. It aims at mathematic description of the droplet flight trajectory, droplet velocity and acceleration. To this end, the droplet flight trajectory was first fitted using the 3rd order polynomial regression and it was found that the model can be reduced to the 2nd order. The average diameter of a droplet, transfer rate of droplets, average velocity and acceleration of a droplet were calculated. The geometric shape factor was estimated. A new metal transfer monitoring method which is based on narrow band filter and does not require He-Ne laser, has been used in this study to observe the metal transfer process.

### 1. INTRODUCTION

The GMAW (Gas Metal Arc Welding) process employs a continuous consumable solid wire electrode and an externally supplied active shielding gas. A scheme of the process is shown in Fig. 1. The consumable wire electrode produces an arc with the workpiece making part of the electric circuit and providing a filler to the weld joint. The wire is fed to the arc by an automatic wire feeder, of which both push and pull-types are employed, depending on the wire composition, diameter, and welding application. The externally supplied shielding gas plays dual roles in the GMAW. First, it protects the arc and the molten or hot, cooling weld metal from the contamination of the air. Second, it provides the desired arc characteristics through its effect on ionization. A variety of gases can be used, depending on the reactivity of the metal being welded, the design of the joint and the specific arc characteristics that are desired.

Metal transfer is the process of the molten metal's movement from the electrode tip to the workpiece, which includes droplet formation, detachment and transfer in the arc gap. The transport of droplets into the weld pool is largely responsible for the finger penetration commonly observed in the fusion zone [1, 2].

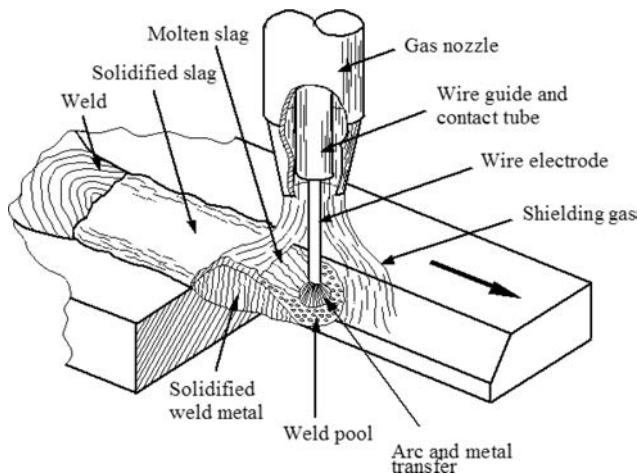


FIG. 1. Illustration of GMAW.

There are a few modes of metal transfer in GMAW such as short circuiting, globular and spray transfer. In the short circuiting transfer the end of the electrode actually touches the molten pool, creating a momentary short circuit. This condition triggers an increase in current sufficient to melt the tip of the electrode and then reestablish the arc between the electrode and the workpiece. The cycle repeats itself about 50 to 250 times per second. This type of transfer is good for welding thin metals in all positions, incomplete fusion may occur in base metal in excess of 3.2 mm. The globular transfer occurs at a current range above short circuiting transfer. The melted droplets that transfer into the molten pool are about two to four times the diameter of the electrode, and they fall in an irregular pattern and with an irregular frequency. This type of transfer typically produces spatters, and in most instances, it is the type of transfer when  $\text{CO}_2$  is the only shielding gas. Spray transfer occurs at high welding currents with argon-rich ( $> 90\%$ ) shielding gas mixtures. The molten droplets are small, and they are forced across the arc in an axial pattern. The arc column is constricted. This type of transfer produces minimal spatter and is conducive to high deposition rates. The rotational spray transfer occurs when a solid wire is used with a long electrode extension of 20 to 40 mm and the shielding gas is a mixture of  $\text{Ar} + \text{CO}_2$  or  $\text{Ar} + \text{O}_2$ . The long electrode extension creates resistance heating of the electrode that causes its end to become molten. Electromechanical forces make the molten end of the electrode rotate in a helical pattern. The shielding gas mixture affects the surface tension of the molten end assisting in the rotational transfer. Deposition rates of 10 to 15 kg/h are attained with this transfer mode [3].

Metal transfer has been a subject matter of many investigations. A better understanding of the metal transfer process is important for improvements in the quality and productivity of welding. The welding voltage, current, arc length,

shielding gas and wire feed rate can all affect the metal transfer process. Among them, current is most often studied for its influence on the droplet size, frequency and acceleration in the arc.

Many papers described the methodology of mathematical analysis for the formation of droplets and analysed and calculated the effects of individual forces acting on metal droplets at the tip of the wire in GMAW [4]. In order to determine the dominant factors, which affect the metal transfer mode, a dimensional analysis has been conducted in previous studies [5]. Several dimensionless numbers which are derived on the basis of the surface-tension force are the Weber ( $W_e$ ), Bond ( $B_o$ ),  $N_{SE}$ ,  $N_{SV}$ . Here the subscripts  $S$  and  $V$  denote the surface tension and viscosity. These numbers represent the relative effects of electrode melting, gravitational, electromagnetic and viscous forces with respect to the surface-tension force, respectively. The  $N_{SE}$  number was found to be the most important dimensionless number influencing the characteristics of metal transfer [5]. Through the arc sensing methods are also widely used to study metal transfer. By recording and analysing fluctuations of the welding voltage and/or current, it is possible to predict the metal transfer mode [6]. Due to its simplicity and nonintrusive nature, through the arc sensing can also be used to study the GMAW process, but can also be used in welding process control. Most of recent investigations focused on studying the effect of waveform parameters on the mode of metal transfer in pulsed gas metal arc welding (GMAW-P) [7–11]. The metal transfer mode is also an interesting subject matter in newly developed welding methods such as double electrode gas metal arc welding (DE-GMAW) developed at the University of Kentucky [12, 13]. Some studies focused on detailed analysis of droplet velocity and developed a model based only on the electromagnetic pinch force [14]. Many efforts have been made to optimize welding parameters to achieve one droplet per pulse (ODPP-GMAW) [15]. Further, a non-isothermal numerical model has been developed to simulate the metal transfer process in GMAW. Experiments with high-speed photography and laser-shadow imaging show that the simulation results were in broad agreement with the actual welding process [16]. The newest investigations about metal transfer even allow to create a new classification of mode of metal transfer modes [17]. The melting of the wire, which is fundamental and influences the process stability and productivity, has also been a main topic of some investigations [18]. Recently, hybrid laser-MIG welding methods have also been studied [19].

Droplet acceleration in the arc has been calculated by many authors [20–25] using the empirical formulation presented by LANCASTER [26]. To calculate the plasma drag force exerted on the droplet using this formulation, the droplet was assumed to have a spherical shape and accelerate to the workpiece with a constant acceleration [27]. The acceleration of the droplet is found to be near constant by JONES *et al.* [28] and assumed to be constant by many authors in their

calculations [20–24]. With many factors influencing metal transfer, theoretical models such as the static force balance theory [29–30] and the pinch instability theory [31–32] have been proposed to explain the metal transfer phenomena, but the success is limited. The authors [33] investigated the relative magnitudes of the detaching forces in static force balance theory and showed good agreement with experimental results within the range of globular transfer; however, in the spray transfer mode, the theory deviates significantly from the experiment.

Despite a significant progress, the existing investigations that have been carried out up to date have not covered the subject matter of mathematic description of droplet flight trajectory, changes of droplet velocity and droplet acceleration, although this subject matter can further our understanding of the metal transfer process. Hence, the droplet size, droplet transfer rate, mathematic descriptions of droplet flight trajectory and droplet velocity and droplet acceleration, are analyzed in this paper. In previous investigations the back-lighting technique has been used to image the metal transfer process using a He-Ne laser [34]. The problem with this method is that the laser and imaging plane must be placed on two opposite sides of the torch. A high-speed camera with a narrowband pass filter is used to directly view the metal transfer process. This technique is easier to use because of the elimination of the need for back-lighting.

## 2. THEORETICAL BACKGROUND

The static force balance theory postulates that the drop detaches from the electrode when the static detaching forces on the drop exceeds the static retaining forces. Four different forces have been considered [33]:

- the gravitational force,
- electromagnetic force,
- plasma drag force,
- surface tension force.

The gravitational force is due to the mass of the drop and acts as a detaching force when welding in flat position:

$$(2.1) \quad F_g = \frac{4}{3}\pi R^3 \rho_D g,$$

where  $R$  – radius of droplet,  $\rho_D$  – density of droplet.

The electromagnetic force on the drop results from divergence or convergence of current flow within the electrode. The electromagnetic force is given by Lorentz's law:

$$(2.2) \quad F_{em} = \bar{J} \times \bar{B},$$

where  $J$  – current density,  $B$  – magnetic flux.

By assuming that the current density on the drop is uniform, the total electromagnetic force on a drop can be obtained by integrating Eq. (2.2) over the current conducting surface of the drop [14]:

$$(2.3) \quad F_m = \frac{\mu_0 I^2}{4\pi} f(s),$$

where  $I$  – welding current,  $\mu_0$  – the magnetic permeability of the free space,  $f(s)$  – a geometric shape factor depending on the droplet radius and neck diameter during droplet growth and detachment.

The plasma drag force on the liquid drop can be estimated by considering the drag force on a sphere immersed in a fluid of uniform velocity field [33]:

$$(2.4) \quad F_d = C_D A_P \left( \frac{\rho_f v_f^2}{2} \right),$$

where  $C_D$  – drag coefficient,  $A_P$  – projected area on the plane perpendicular to the fluid flow,  $\rho_f$  – density of the fluid,  $v_f$  – velocity of the gas.

Surface tension force, which acts to retain the liquid drop on the electrode is given as follows:

$$(2.5) \quad F_S = 2\pi\alpha\gamma,$$

where  $\alpha$  – radius of the electrode,  $\gamma$  – surface tension of the liquid.

From the static force balance theory, the droplet size can be calculated under the assumption that the drop is not detached from electrode if the sum of detaching forces equals the retaining force [33]:

$$(2.6) \quad F_\gamma = F_{em} + F_g + F_d.$$

Hence, Eq. (2.6) holds during the process of droplet formation. After the droplet is detached, it travels in the arc gap subjecting the sum of the following forces:

$$(2.7) \quad F_{em} + F_g + F_{arc},$$

where  $F_{arc}$  accounts all other possible forces except for the electromagnetic and gravitational forces. To calculate the geometric shape factor  $f(s)$  defined in (2.3), the other forces are omitted. Hence,

$$(2.8) \quad \frac{4}{3}\pi R^3 \rho_D a = \frac{\mu_0 I^2}{4\pi} f(s) + \frac{4}{3}\pi R^3 \rho_D g,$$

where  $a$  is the acceleration of the droplet in the air gap. As a result, the geometric shape factor can be calculated as:

$$(2.9) \quad f(s) = \frac{\frac{16}{3}\pi^2 R^3 \rho_D (a - g)}{\mu_0 I^2}.$$

## 3. EXPERIMENTAL SETUP AND PROCEDURE

Mild steel Quantum ARC 6 carbon steel wire (AWS A5.18, ER70S-6) equivalent to SG2 was used in the experiments. The electrode's diameter is 1.2 mm (0.045 inch). The chemical composition of the wire is given in Table 1. The shielding gas used was pure argon.

**Table 1. Chemical composition of wire.**

C	Mn	Si	P	S	Cu
0.06–0.15	1.40–1.85	0.8–1.15	<0.025	<0.025	<0.05

Experiments were carried out on an automated GMAW platform. A simple scheme of the experimental setup with data flow is shown in Fig. 2. The torch was moved while the work-piece was in a fixed position such that the camera was stationary in relation to the work-piece. All welds were made with a standard water cooled welding gun Miller Roughneck C 4015. The wire feeder was a Miller R-115. The torch was moved at the travel speed of 25 cm/min (10 inch/min) to make bead-on-plate welds. Direct current levels between 206 and 262 A were examined, all at an operating voltage 32 V. All experiments were carried out with a tip-to-work distance of 15 mm. The current and, therefore, the metal transfer mode were changed by changing the wire feed rates in the range from 4.57 m/min to 6.85 m/min (180 to 270 inch/min). The conventional three-phase welding machine Hobart EXCEL – ARC 8065 CC/CV was used.

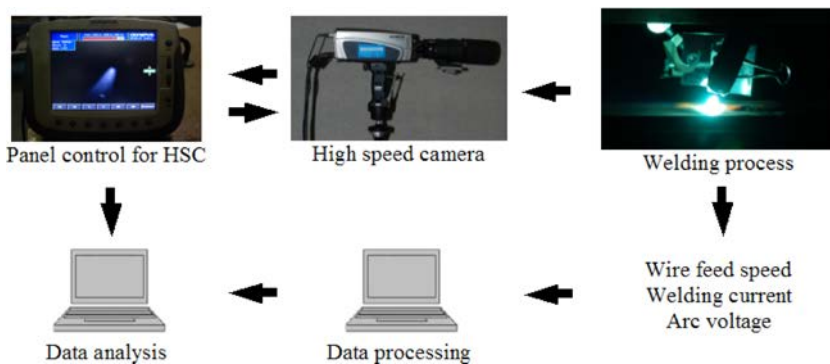


FIG. 2. Experimental setup with flow of data.

During welding the arc voltage, welding current and wire feed speed were continuously measured. Electrical current was measured by Hall effect current sensor Model CLN-500. The voltage was measured by a resistance bridge directly in the output of power supply. Signals from the welding circuit were recorded on the PC through the data acquisition card NI DAQ 6036E. Analysis of the metal

transfer process was performed using high speed camera Olympus i-SPEED at 3000 frame per second (fps). The camera direction was perpendicular to the welding direction. In addition to an aperture of 11 and a shutter of 1, a narrow-band filter (central wavelength 685 nm, bandwidth 20 nm) was used to reduce the arc brightness in order to image the metal transfer.

#### 4. RESULTS AND DISCUSSION

The recorded images of metal transfer from the high speed camera are analyzed by i-SPEED viewer and IrfanViewer software. An image sequence of droplet track in GMAW for wire feed speed 270 inch/min – welding current 262 A and arc voltage 32 V at 3000 frames per second, is shown in Fig. 3; and for wire feed speed 180 inch/min – welding current 206 A in Fig. 4. The arrow marks the same droplet being tracked. Experiments were performed on clean plates. The macroscopic examination of padding welds with welding parameters are given in Table 2.

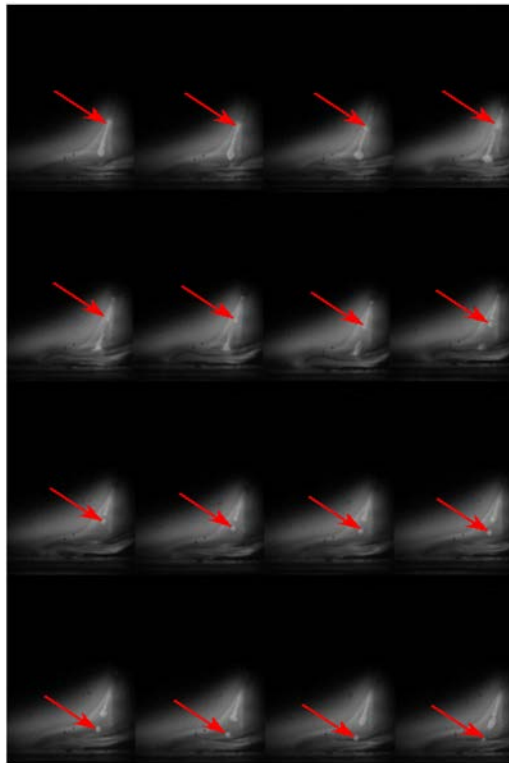


FIG. 3. Image sequence of droplet track in GMAW. Wire speed 270 inch/min (6.85 m/min) – welding current 262 A, arc voltage 32 V, 100% Ar. Sampling speed is 3000 frames per second. The arrow marks the same droplet.

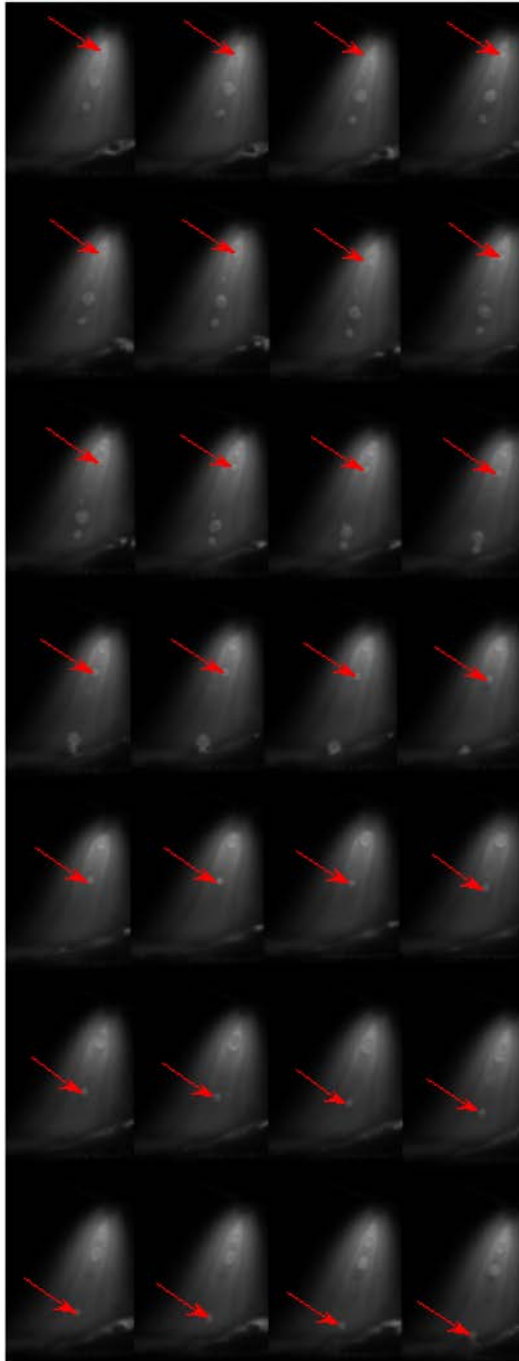
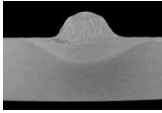
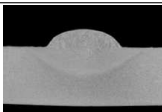
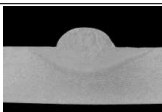
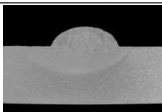
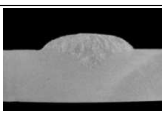
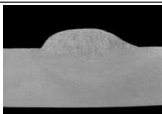
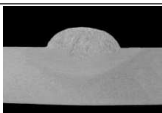


FIG. 4. Image sequence of droplet track in GMAW. Wire speed 180 inch/min (4.57 m/min) – welding current 206 A, arc voltage 32 V, 100% Ar. Sampling speed is 3000 frames per second. The arrow marks the same droplet.

**Table 2. Macroscopic examination of padding welds.**

No	Wire feed speed [inch/min]/[m/min] welding current [A] and standard deviation $I \pm S_{dI}$	Appearance	Macroscopic Section 1:1
1	180/4.57 206 ± 19		
2	190/4.83 211 ± 33		
3	200/5.08 216 ± 12		
4	210/5.33 225 ± 7		
5	220/5.59 229 ± 5		
6	230/5.84 232 ± 4		
7	240/6.10 247 ± 7		
8	250/6.35 250 ± 3		
9	260/6.60 256 ± 8		
10	270/6.85 262 ± 5		

#### 4.1. Droplet diameter and number of droplets per second

The first goal of this study was to calculate the diameter of the droplet. To this end, it was necessary to measure droplet diameter in two directions (horizontal  $d_h$  and vertical  $d_v$  diameter), as shown in Fig. 5. When the droplet to be analyzed reaches a particular location in the image, the diameter  $D$  of the droplet is calculated as:

$$(4.1) \quad D = \frac{(d_h + d_v)}{2}.$$

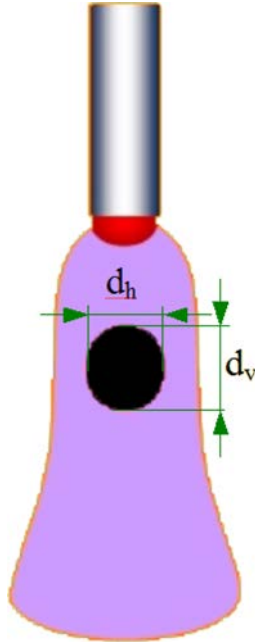


FIG. 5. Methodology for calculating the diameter of a single droplet in GMAW;  $d_h$  – horizontal diameter,  $d_v$  – vertical diameter.

The average diameter was calculated for each set of welding parameters using seven image sequences. The minimal and maximal values were not used in the calculation. Next sequence was used if the difference between horizontal and vertical diameter was higher than 20%. The standard error of droplet diameter was calculated based on the following formula:

$$(4.2) \quad S_D = \sqrt{S_d^2 + S_i^2},$$

where  $S_D$  – standard error of droplet diameter,  $S_d$  – standard deviation,  $S_i$  – measurement resolution.

The measurement resolution was  $S_i = 0.1$  mm. The results of calculation are given in Table 3. To calculate the transfer rate, the following assumptions were made:

- the difference between horizontal and vertical diameter is less than 20%, and the droplet can be assumed to be spherical approximately,
- the welding process is stable and transfer rate is constant vs. time,
- spatters are negligible.

**Table 3. Relationship between wire feed speed and droplet diameter.**

No	Wire feed [inch/min]	Mean value of $d_v/d_h$ [%]	Standard deviation $S_d$ [mm]	Real value with standard error $D \pm S_D$ [mm]
1	180	101.86	0.12	0.99±0.16
2	190	110.08	0.12	0.90±0.16
3	200	105.07	0.06	0.82±0.12
4	210	93.36	0.07	0.68±0.12
5	220	100.41	0.08	0.65±0.13
6	230	101.23	0.12	0.52±0.15
7	240	96.54	0.12	0.51±0.15
8	250	103.08	0.06	0.48±0.12
9	260	102.16	0.02	0.46±0.10
10	270	99.81	0.03	0.43±0.10

The second goal was to calculate the droplet transfer rate (the number of droplets detached per second). In a unit time, the total volume of the transferred droplets is equal to the molten metal:

$$(4.3) \quad n \frac{4}{3} \pi \left( \frac{D}{2} \right)^3 = \frac{1}{4} \pi d^2 v_{el},$$

where  $n$  – number of droplets per second,  $D$  – average diameter of droplet [m],  $V_{el}$  – wire feed [m/s].

The number of droplets can thus be calculated as:

$$(4.4) \quad n = \frac{3}{8} \cdot \frac{d^2}{D^3} \cdot v_{el}.$$

The results of the transfer rate calculation are shown in Fig. 6 for wire feed rate in the range from 180 inch/min to 270 inch/min with volume of droplet.

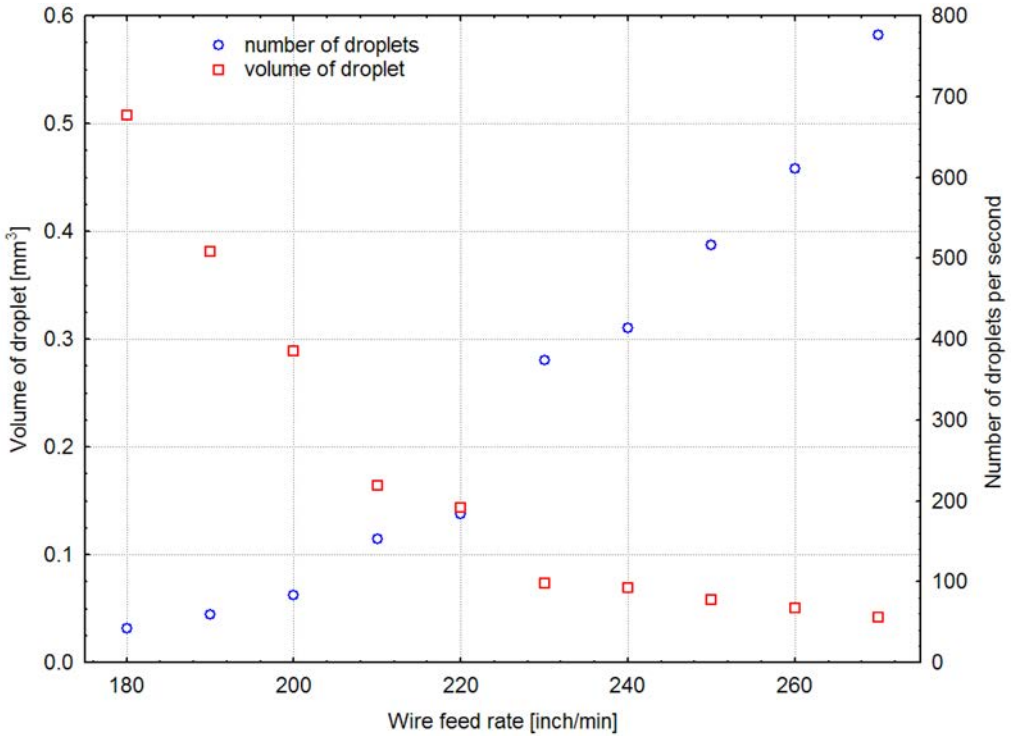


FIG. 6. Influence of wire speed rate (welding current) on droplet volume and transfer rate.

#### 4.2. Droplet velocity and acceleration

The authors first used a 3rd degree polynomial to fit the travel of the droplet:

$$(4.5) \quad y(t) = A + B_1 \cdot t + B_2 \cdot t^2 + B_3 \cdot t^3,$$

where  $t$  – time [ms],  $y$  – distance traveled along the arc axis after detachment [mm],  $A$ ,  $B_i$  – coefficients.

The resultant coefficients fitted with the residual are given in Table 4.

Since the residual in all cases is relatively small, a reduced model of 2nd degree is considered:

$$(4.6) \quad y(t) = A + B_1 \cdot t + B_2 \cdot t^2.$$

The resultant coefficients and residuals are given in Table 5 for wire feed rate in the range from 180 inch/min to 270 inch/min. As it can be seen, the residuals are still small and are in the range of acceptable error. Hence, the 2nd

**Table 4. Calculated coefficients in formula 4.5 in relation to wire feed rate.**

No	Wire feed rate [inch/min]	$A$	$B_1$	$B_2$	$B_3$	$\varepsilon$ [mm]
1	180	0.01114	0.24233	0.07043	-0.00021	0.1141
2	190	0.00672	0.15328	0.07731	-0.00117	0.0556
3	200	-0.00651	0.20726	0.06304	-0.00115	0.0473
4	210	0.10272	0.19594	0.06292	-0.00014	0.0615
5	220	-0.02921	0.12451	0.07911	-0.00139	0.1726
6	230	-0.05401	0.54832	-0.11971	0.01942	0.0592
7	240	0.10203	0.38482	0.02997	-0.00049	0.0428
8	250	0.03580	0.17848	0.10762	-0.00688	0.0410
9	260	-0.03676	0.48401	0.13222	-0.01175	0.0418
10	270	-0.10866	0.85462	-0.03029	0.009	0.0566

**Table 5. Calculated coefficients in formula 4.6 in relation to wire feed rate.**

No	Wire feed rate [inch/min]	$A$	$B_1$	$B_2$	$\varepsilon$ [mm]
1	180	0.00363	0.25293	0.06754	0.1138
2	190	-0.02305	0.20089	0.06274	0.1489
3	200	-0.03243	0.25064	0.04921	0.0495
4	210	0.10624	0.19032	0.06462	0.0457
5	220	-0.06465	0.18118	0.06176	0.2230
6	230	0.19185	0.04307	0.07449	0.1132
7	240	0.09091	0.40344	0.02403	0.0444
8	250	-0.08189	0.39559	0.03193	0.0639
9	260	-0.09613	0.65459	0.04412	0.0448
10	270	-0.04073	0.68622	0.04618	0.0639

degree polynomial model can be accepted. The resultant models of 2nd degree are graphically shown in Fig. 7.

To calculate the changes in velocity  $v_i$  for wire feed speed in the range of 180 inch/min to 270 inch/min, the derivative of movement equation (4.6) can be calculated. To achieve droplet velocity in unit of mm/s formula (4.6) was multiplication by 1000 times. The results of the calculation are shown in Fig. 8.

To calculate the average droplet velocity, the following formula was used:

$$(4.7) \quad \bar{v}_i = \frac{1}{T} \int_0^T v_i(t) dt,$$

where  $T$  is the time the droplet reaches the weld pool. To calculate the droplet acceleration, the 2nd derivative of movement equation was calculated:

$$(4.8) \quad \ddot{y}(t) = 2 \cdot B_2.$$

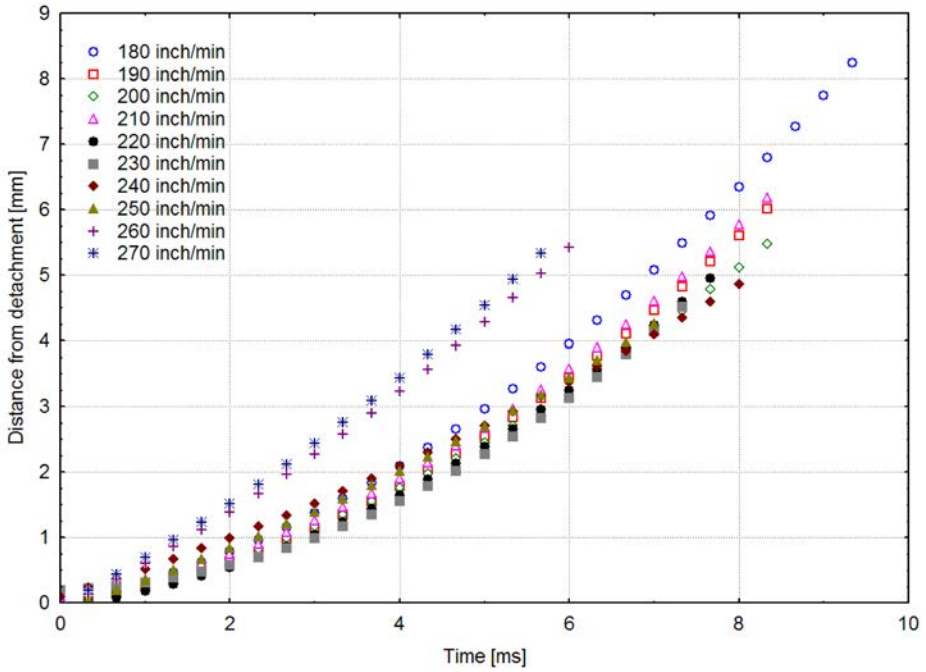


FIG. 7. Influence of wire speed rate (welding current) on droplet flight trajectory.

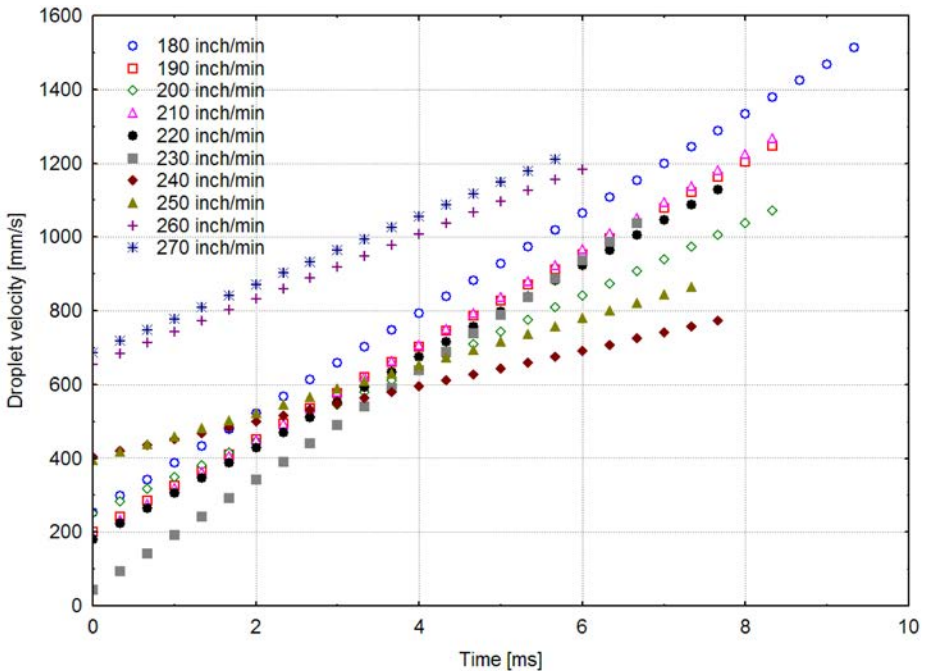


FIG. 8. Influence of wire speed rate (welding current) on droplet velocity vs. time.

The results of average droplet velocity and acceleration are given in Table 6.

**Table 6. The average droplet velocity and droplet acceleration.**

No	Wire feed rate [inch/min]	Average velocity [mm/s]	Average acceleration [ $m/s^2$ ]
1	180	883.30	135.08
2	190	723.72	125.48
3	200	660.64	98.40
4	210	728.82	129.24
5	220	645.67	123.52
6	230	539.67	148.98
7	240	587.67	48.06
8	250	629.74	63.86
9	260	919.31	88.24
10	270	947.90	92.36

#### 4.3. Geometric shape factor

Based on formula (2.9), results of droplet diameter in Table 3, and droplet acceleration in Table 6, the geometric shape factor has been calculated. The relationship between droplet diameter and geometric shape factor is shown in Fig. 9.

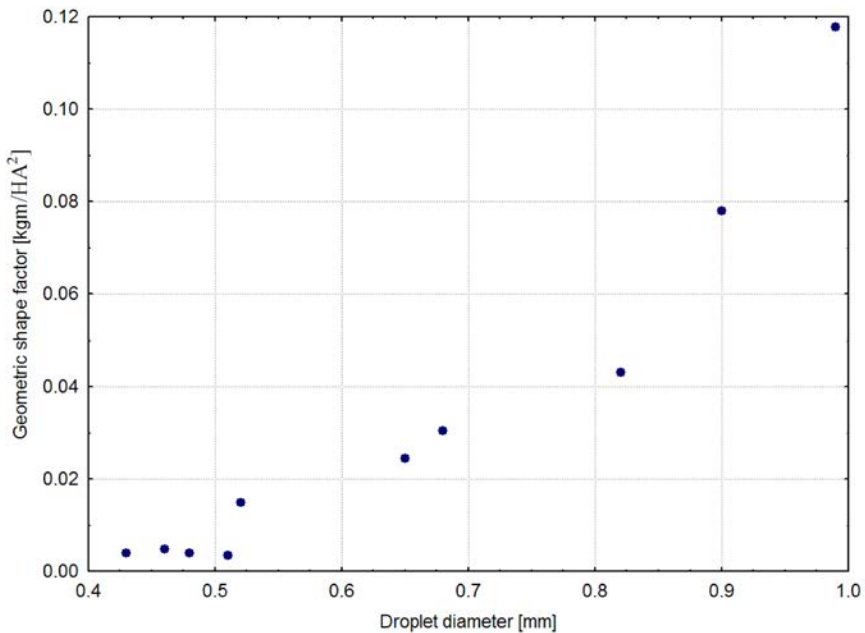


FIG. 9. Influence of droplet diameter (determined by the wire speed rate or welding current) on geometric shape factor  $f(s)$ .

As can be seen in Fig. 8, the geometric shape factor of a droplet strongly depends on the droplet diameter and increases as the droplet diameter increases.

## 5. CONCLUSION

In this paper, measurement data of metal transfer has been obtained from the GMAW process in the range of welding wire speed from 180 inch/min to 270 inch/min. The authors can conclude:

1. Measurement of the droplet diameter has shown that average diameter of droplet in the range of wire feed rate from 180 to 270 inch/min changes in the range from  $0.99 \pm 0.16$  mm to  $0.43 \pm 0.10$  mm.
2. The results of calculated the drop frequency (droplet transfer rate) is in the range from 42 to 776 droplets per second.
3. To fit the droplet flight trajectory, a 2nd degree polynomial is adequate.
4. To calculate drop velocity, the first order derivative of the fitted quadratic curves of drop trajectory was calculated. The average drop velocity in the range of wire feed rate from 180 to 270 inch/min varies from 883.30 to 947.90 mm/s.
5. To calculate the drop acceleration, the second order derivative of the fitted quadratic curves of drop trajectory was calculated. The acceleration is constant for each wire feed speed and in the range of 48.06 to 148.98  $\text{m/s}^2$ .
6. The geometric shape factor of the droplet was calculated. This coefficient depends on the droplet radius and varies from 0.0039 to 0.1178 for the droplet diameter in the range from 0.43 to 0.99 mm.

The experience gained would allow the authors to determine further directions on metal transfer research and use the simple method proposed in this study to on-line monitor the welding process in automated GMAW.

## ACKNOWLEDGEMENTS

The authors would like to thank the Fulbright Commission for financing this research, which was done within the framework of the research project Young Advanced Research Grant – University of Kentucky Centre for Manufacturing, Welding Research and Development Laboratory and the Applied Machine Vision Laboratory 2007–2008. This research is also supported in part by the National Science Foundation under grant CMMI-0726123.

## REFERENCES

1. R. W. MESSLER, *Principles of Welding, Processes, Physics, Chemistry, and Metallurgy*, Ch. 3, John Wiley & Sons, New York 1999.
2. R. L. O'BREIN, *Welding Handbook, vol. 2 Welding processes*, American Welding Society, Miami 1991.
3. Welding Workbook: *Gas Metal Arc Welding, Transfer Modes*, Datasheet No 202a, Welding Journal, **76**, 2, 57–58, 1997.
4. J. HAIDAR, *An analysis of the formation of metal droplets in arc welding*, Journal of Physics D: Applied Physics, **31**, 10, 1233–1244, 1998.
5. S. K. CHOI, Y. S. KIM, C. D. YOO, *Dimensional analysis of metal transfer in GMA welding*, Journal of Physics D: Applied Physics, **32**, 3, 326–334, 1999.
6. J. A. JOHNSON, N. M. CARLSON, H. B. SMARTT, D. E. CLARK, *Process control of GMAW: sensing of metal transfer mode*, Welding Journal, **70**, 4, 91–99, 1991.
7. C. S. WU, M. A. CHEN, Y. F. LU, *Effect of current waveforms on metal transfer in pulsed gas metal arc welding*, Measurement Science and Technology, **16**, 12, 2459–2465, 2005.
8. G. WANG, G. HUANG, Y. M. ZHANG, *Numerical analysis of metal transfer in gas metal arc welding under modified pulsed current conditions*, Metallurgical and Materials Transactions B, **35B**, 5, 857–866, 2004.
9. N. JACOBSEN, *Monopulse investigation of drop detachment in pulsed gas metal arc welding*, Journal of Physics D: Applied Physics, **25**, 5, 783–797, 1992.
10. P. K. GHOSH, L. DORN, M. HÜBNER, V. K. GOYAL, *Arc characteristics and behaviour of metal transfer in pulsed current GMA welding of aluminium alloy*, Journal of Materials Processing Technology, **194**, 1–3, 163–175, 2007.
11. S. K. CHOI, C. D. YOO, Y. S. KIM, *The dynamic analysis of metal transfer in pulsed current gas metal arc welding*, Journal of Physics D: Applied Physics, **31**, 2, 207–215, 1998.
12. K. LI, Y. M. ZHANG, *Metal Transfer in Double-Electrode Gas Metal Arc Welding*, Journal of Manufacturing Science and Engineering-Transactions of the ASME, in print.
13. Z. Z. WANG, Y. M. ZHANG, *Image processing algorithm for automated monitoring of metal transfer in double-electrode GMAW*, Measurement Science and Technology, **18**, 7, 2048–2058, 2007.
14. Q. LIN, X. LI, S. W. SIMPSON, *Metal transfer measurements in gas metal arc welding*, Journal of Physics D: Applied Physics, **34**, 3, 347–353, 2001.
15. P. K. PALANI, N. MURUGAN, *Selection of parameters of pulsed current gas metal arc welding*, Journal of Materials Processing Technology, **172**, 1, 1–10, 2006.
16. F. WANG, W. K. HOU, S. J. HU, *Modelling and analysis of metal transfer in gas metal arc welding*, Journal of Physics D: Applied Physics, **36**, 9, 1143–1152, 2003.
17. D. IORDACHESCU, L. QUINTINO, *Steps toward a New Classification of Metal Transfer in Gas Metal Arc Welding*, Journal of Materials Processing Technology, in press.
18. P. J. MODENESI, R. I. REIS, *A model for melting rate phenomena in GMA welding*, Journal of Materials Processing Technology, **189**, 1–3, 199–205, 2007.

19. G. CAMPANA, A. FORTUNATO, A. ASCARI, G. TANI, L. TOMESANI, *The influence of arc transfer mode in hybrid laser-MIG welding*, Journal of Materials Processing Technology, **191**, 1–3, 111–113, 2007.
20. C. H. KIM, W. ZHANG, T. DEBROY, *Modeling of Temperature Field and Solidified Surface Profile During Gas-Metal Arc Fillet Welding*, Journal of Applied Physics, **94**, 4, 2667–2679, 2003.
21. H. G. FAN, R. KOVACEVIC, *Droplet Formation, Detachment, and Impingement on the Molten Pool in Gas Metal Arc Welding*, Metall. Mater. Trans. B, **30B**, 4, 791–801, 1999.
22. H. G. FAN, R. KOVACEVIC, *A Unified Model of Transport Phenomena in Gas Metal Arc Welding including Electrode, Arc Plasma and Molten Pool*, Journal of Physics D: Applied Physics, **37**, 18, 2531–2544, 2004.
23. S. SUBRAMANIAM, D. R. WHITE, D. J. SCHOLL, W. H. WEBER, *In Situ Optical Measurement of Liquid Drop Surface Tension in Gas Metal Arc Welding*, Journal of Physics D: Applied Physics, **31**, 16, 1963–1967, 1998.
24. Y. WANG, H. L. TSAI, *Impingement of Filler Droplets and Weld Pool Dynamics During Gas Metal Arc Welding Process*, International Journal of Heat and Mass Transfer, **44**, 11, 2067–2080, 2001.
25. Y. WANG, H. L. TSAI, *Effects of Surface Active Elements on Weld Pool Fluid Flow and Weld Penetration in Gas Metal Arc Welding*, Metallurgical and Materials Transactions B, **32B**, 3, 501–515, 2001.
26. J. F. LANCASTER, *The Physics of Welding*, 2nd ed., Pergamon, Oxford 1986.
27. J. HU, H. L. TSAI, *Metal Transfer and Arc Plasma in Gas Metal Arc Welding*, Journal of Heat Transfer, **129**, 8, 1025–1035, 2007.
28. L. A. JONES, T. W. EAGAR, J. H. LANG, *A Dynamic Model of Drops Detaching from a Gas Metal Arc Welding Electrode*, Journal of Physics D: Applied Physics, **31**, 107–123, 1998.
29. J. C. AMSON, *An analysis of the gas shielded consumable metal arc welding system*, British Welding Journal, **41**, 4, 232–249, 1962.
30. J. H. WASZNIK, L. H. J. GRAAT, *Experimental investigation of the forces acting on a drop of weld metal*, Welding Journal, **62**, 4, 109–116, 1983.
31. C. J. ALLUM, *Metal transfer in arc welding as a varicose instability: Part 1 – varicose instability in a current-carrying liquid cylinder with surface charge*, Journal of Physics D: Applied Physics, **18**, 7, 1431–1446, 1985.
32. C. J. ALLUM, *Metal transfer in arc welding as a varicose instability: Part 2 – development of model for arc welding*, Journal of Physics D: Applied Physics, **18**, 7, 1447–1468, 1985.
33. Y. S. KIM, T. W. EAGER, *Analysis of Metal Transfer in Gas Metal Arc Welding*, Welding Journal, **72**, 6, 296–278, 1993.
34. C. D. ALLEMAND, R. SCHOEDER, D. E. RIES, T. W. EAGER, *A method of filming metal transfer in welding arcs*, Welding Journal, **64**, 1, 45–47, 1985.

*Received February 12, 2008; revised version June 2, 2008.*

---